Observation of a Nonclassical Berry's Phase for the Photon

Paul G. Kwiat and Raymond Y. Chiao
Department of Physics, University of California, Berkeley, California 94720
(Received 5 July 1990)

Coincidence detection of photon pairs produced in parametric fluorescence, in conjunction with a Michelson interferometer in which one member of each pair acquired a geometrical phase due to a cycle in polarization states, has allowed the first observation of Berry's phase at the single-photon level. We have verified that each interfering photon was essentially in an $n=1$ Fock state, by means of a beam splitter following the interferometer combined with a triple-coincidence technique. The results can be interpreted in terms of a nonlocal collapse of the wave function.

PACS numbers: 42.50.Bs, 03.65.Bz, 42.65.Ky

Quantum interference possesses global geometrical features, which spring from the metrical properties of Hilbert space. One such feature is Berry's phase,[1] which can be acquired by a quantum system whenever it evolves adiabatically and cyclically back to its initial state. Simon[2] made a connection between Berry's phase and the geometry of fiber bundles. Aharonov and Anandan[3] generalized this geometrical phase to nonadiabatic evolutions. Berry's phase has manifestations which range from low-energy physics, e.g., in fiber optics,[4] to high-energy physics, e.g., in chiral anomalies of gauge-field theories.[5]

In its optical manifestations, Berry's phase has appeared so far only on the classical level, as a phase shift of a classical electromagnetic wave.[4,6-10] There has been a controversy as to whether one should view optical Berry's phases as originating from the quantum or the classical level.[4,11-14] Here we point out that there can exist nonclassical manifestations of this phase when the state of the light is nonclassical. Using an entangled state of light, we have observed on the quantum level one form of Berry's phase, Pancharatnam's phase,[6-10] which is generated after a cycle of polarization states. We believe that this experiment will settle the controversy.

In our experiment the incident light was prepared in an entangled state consisting of a pair of photons whose energies, although individually broad in spectrum, sum up to a sharp quantity E because they were produced from a single photon whose energy E was sharp. This entangled state is given by

$$|\Psi\rangle_{\text{in}} = \int dE' A(E') |1\rangle_{E'} |1\rangle_{E-E'}, \quad (1)$$

where $A(E') = A(E-E')$ is the complex probability amplitude for finding one photon with an energy E', i.e., in the $n=1$ Fock state $|1\rangle_{E'}$, and one photon with an energy $E-E'$, i.e., in the $n=1$ Fock state $|1\rangle_{E-E'}$. According to the standard Copenhagen interpretation, the meaning of this entangled state is that when a measurement of the energy of one photon results in a sharp value E', there is a sudden collapse of the wave function such that instantly at a distance, the other photon, no matter how remote, also possesses a sharp value of energy $E-E'$. Thus energy is conserved. Entangled states, i.e., coherent sums of product states, such as the one given by Eq. (1), result in Einstein-Podolsky-Rosen-like effects which are nonclassical and nonlocal.[15]

We prepared the entangled state of energy, Eq. (1), by means of parametric fluorescence in the $\chi^{(2)}$ nonlinear optical crystal potassium dihydrogen phosphate (KDP), excited by a single-mode ultraviolet (uv) argon-ion laser operating at $\lambda = 351.1$ nm.[16] The uv laser beam was normally incident on the KDP input face. In this fluorescence process, a single uv photon with a sharp spectrum is spontaneously converted inside the crystal into two photons ("signal" and "idler") with broad, conjugate spectra centered at twice the uv wavelength, conserving energy and momentum. We employed type-I phase matching, so that both signal and idler beams were horizontally polarized. Coincidences in the detection of conjugate photons were then observed. The KDP crystal was 10 cm long and cut such that the c axis was 50.3° to its input face. We selected for study signal and idler beams both centered at $\lambda = 702.2$ nm which emerged at $-1.5°$ and $+1.5°$, respectively, with respect to the uv beam.

In Fig. 1, we show a schematic of the experiment. The idler photon (upper beam) was transmitted through the "remote" filter $F1$ to the detector $D1$, which was a cooled RCA C31034A-02 photomultiplier. The signal photon (lower beam) entered a Michelson interferometer, inside one arm of which were sequentially placed two zero-order quarter-wave plates $Q1$ and $Q2$. The fast axis of the first wave plate $Q1$ was fixed at 45° to the horizontal, while the fast axis of the second wave plate $Q2$ was slowly rotated by a computer-controlled stepping motor. After leaving the Michelson interferometer the signal beam impinged on a second beam splitter $B2$, where it was either transmitted to detector $D2$ through filter $F2$, or reflected to detector $D3$ through filter $F3$. Filters $F2$ and $F3$ were identical: They both had a broad bandwidth of 10 nm centered at 702 nm. Detec-

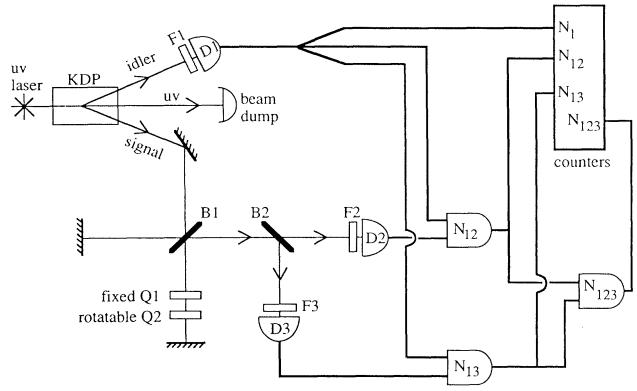

FIG. 1. Schematic of experiment to observe an optical Berry's phase on the quantum level. $D1$, $D2$, and $D3$ are photomultipliers, $Q1$ and $Q2$ quarter-wave plates, and $B1$ and $B2$ beam splitters. Logical AND symbols denote coincidence detectors.

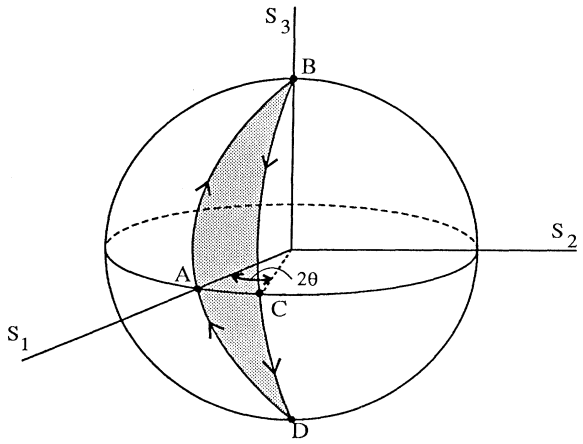

FIG. 2. Generalized Poincaré sphere, where S_1, S_2, and S_3 are Stokes parameters. Circuit $ABCDA$ represents a round trip through wave plates $Q1$ and $Q2$, where θ is the angle between their fast axes. Berry's phase, here Pancharatnam's phase, is 2θ for this circuit.

tors $D2$ and $D3$ were essentially identical to $D1$. Coincidences between $D1$ and $D2$ and between $D1$ and $D3$ were detected by feeding their outputs into constant-fraction discriminators and coincidence detectors after appropriate delay lines. We used EGG C102B coincidence detectors with coincidence window resolutions of 1.0 and 2.5 ns, respectively. Also, triple coincidences between $D1$, $D2$, and $D3$ were detected by feeding the outputs of the two coincidence counters into a third coincidence detector (a Tektronix 11302 oscilloscope used in a counter mode). The various count rates were stored on a computer every second.

Our particular arrangement of quarter-wave plates in the Michelson interferometer has been shown previously to generate Pancharatnam's phase on the *classical* level.[7,8] Upon appropriate detection after the interferometer, we observed at the *quantum* level the interference fringes resulting from this phase. To calculate the phase, we use the generalized Poincaré sphere[9,10] shown in Fig. 2, where polarization states are referred to space-fixed axes, and not to the direction of light propagation, as in the ordinary Poincaré sphere. (We do so in order to avoid extraneous discontinuities upon reflection from mirrors.) The first quarter-wave plate $Q1$ converts horizontal linear polarization, represented by point A on the equator of the sphere, into circular polarization, represented by B at the North Pole. This transformation of polarizations is represented by a geodesic arc AB. Then $Q2$ converts the circular polarization back to linear polarization (C on the equator), but with an axis rotated from the horizontal by θ, the angle between the fast axes of $Q2$ and $Q1$, in real space. On the sphere, the azimuthal angle from A to C is 2θ. After reflection from the mirror, the linear polarization is unchanged with respect to space-fixed axes, and is again represented on the generalized Poincaré sphere by the same point C. After reentering $Q2$, this is converted to circular polarization represented by D (the south pole), completing geodesic arc BCD. Then $Q1$ reconverts the circular polarization back to horizontal linear polarization, generating geodesic arc DA. Thus a cycle in polarization states is completed, represented by the circuit $ABCDA$. Pancharatnam's phase is minus one-half the solid angle subtended by the circuit with respect to the center of the sphere.[6-10] For this circuit, the phase is equal to 2θ.

We took data both outside and inside the white-light fringe region where the usual interference in singles detection occurs. We report here only on data taken outside this region, where the optical-path-length difference was at a fixed value much greater than the coherence length of the signal photons determined by the filters $F2$ and $F3$. Hence the fringe visibility seen by detectors $D2$ and $D3$ in singles detection was essentially zero.

Here we present a simplified quantum analysis of this experiment. Elsewhere we will present a more comprehensive analysis based on Glauber's correlation functions. The state of the light after the Michelson interferometer is given by

$$|\Psi\rangle_{\text{out}} = \int dE' A(E') |1\rangle_{E'} |1\rangle_{E-E'} \{1 + \exp[i\phi(E-E')]\}/2^{1/2}, \quad (2)$$

where $\phi(E-E') = 2\pi\Delta L/\lambda_{E-E'} + \phi_{\text{Berry}}$ is the phase shift arising from the optical-path-length difference ΔL of the Michelson for the photon with energy $E-E'$, plus the Berry's phase contribution for this photon. The coincidence rate N_{12} (N_{13}) between detectors $D1$ and $D2$ ($D1$ and $D3$) is proportional to the probability of finding at the same time t one photon at detector $D1$ placed at $\mathbf{r}_1$ and one photon at detector $D2$ ($D3$) placed at $\mathbf{r}_2$ ($\mathbf{r}_3$). When a narrow-band

filter $F1$ centered at energy E' is placed in front of the detector $D1$, N_{12} becomes proportional to

$$|\psi'_{\text{out}}(\mathbf{r}_1,\mathbf{r}_2,t)|^2=|\langle \mathbf{r}_1,\mathbf{r}_2,t|\psi\rangle'_{\text{out}}|^2\propto 1+\cos\phi\,, \qquad (3)$$

where the prime denotes the output state after a von Neumann projection onto the eigenstate associated with the sharp energy E' upon measurement. Therefore, the phase ϕ is determined at the sharp energy $E-E'$. In practice, the energy width depends on the bandwidth of the filter $F1$ in front of $D1$, so that the visibility of the fringes seen in coincidences should depend on the width of this *remote* filter. This fringe visibility will be high, provided that the optical-path-length difference of the Michelson interferometer does not exceed the coherence length of the *collapsed* signal-photon wave packet, determined by $F1$. If a sufficiently broadband remote filter $F1$ is used instead, such that the optical-path-length difference is much greater than the coherence length of the collapsed wave packet, then the coincidence fringes should disappear.

In Fig. 3, we show data which confirm these predictions. In the lower trace (squares) we display the coincidence count rate between detectors $D1$ and $D3$, as a function of the angle θ between the fast axes of wave plates $Q1$ and $Q2$, when the remote filter $F1$ was narrow, i.e., with a bandwidth of 0.86 nm. The calculated coherence length of the collapsed signal-photon wave packet (570 μm) was greater than the optical-path-length difference at which the Michelson interferometer was set (220 μm). The visibility of the coincidence fringes was quite high, viz., 60% $\pm$ 5%.[17] This is in contrast to the low visibility, viz., less than 2%, of the singles fringes detected by $D3$ alone (not shown). For comparison, in the upper trace (triangles) we display the coincidence count rate versus θ when a broad remote filter $F1$, i.e., one with a bandwidth of 10 nm, was substituted for the narrow one. The coherence length of the collapsed signal-photon wave packet was thus only 50 μm. The coincidence fringes in this case have indeed disappeared, as predicted.

In light of the observed violations of Bell's inequalities,[18] it is incorrect to interpret these results in terms of an ensemble of conjugate signal and idler photons which possess definite, but unknown, conjugate energies before filtering and detection. Any observable, e.g., energy or momentum, should not be viewed as a local, realistic property carried by the photon *before it is actually measured.*

The function of the second beam splitter $B2$ was to verify that the signal beam was composed of photons in an $n=1$ Fock state. In such a state, the photon, due to its indivisibility, will be either transmitted or reflected at the beam splitter, but not both. Thus coincidences between $D2$ and $D3$ should never occur, except for rare accidental occurrences of two pairs of conjugate photons within the coincidence window. However, if the signal beam were a classical wave, then one would expect an equal division of the wave amplitude at the 50% beam splitter, and hence frequent occurrences of coincidences. An inequality, which was strongly violated in our experiment, places a lower bound on this coincidence rate for classical light (see below). This verifies the essentially $n=1$ Fock state nature of the light, and confirms the previous result of Hong and Mandel.[19]

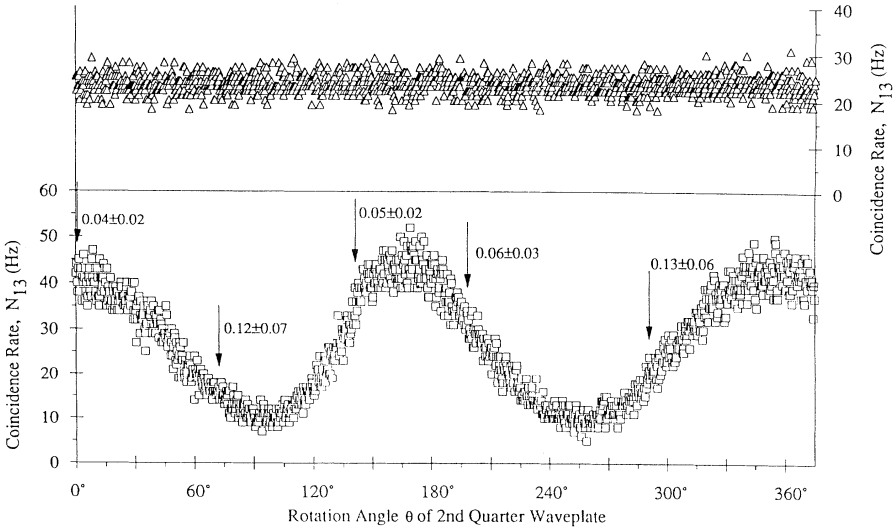

FIG. 3. Interference fringes (lower trace, squares) for an unbalanced Michelson interferometer with a slowly varying Berry's phase, observed in coincidences between $D3$ and $D1$ with a narrow remote filter $F1$. With a broad $F1$, these fringes disappear (upper trace, triangles). They also disappear when detected by $D3$ alone. Vertical arrows indicate where the anticorrelation parameter a was measured (see text).

The vertical arrows in Fig. 3 indicate the points at which triple coincidences were measured. Let us define the anticorrelation parameter[20]

$$a \equiv N_{123} N_1 / N_{12} N_{13}, \quad (4)$$

where N_{123} is the rate of triple coincidences between detectors $D1$, $D2$, and $D3$, N_{12} is the rate of double coincidences between $D1$ and $D2$, N_{13} is the rate of double coincidences between $D1$ and $D3$, and N_1 is the rate of singles detections by $D1$ alone. The inequality $a \geq 1$ has been shown to hold for any classical wave theory.[20] The equality $a = 1$ holds for coherent states $|\alpha\rangle$, independent of their amplitude α. Since in our experiment the amplitude fluctuations in the double-coincidence pulses led to a triple-coincidence detection efficiency η less than unity, we should reduce the expected value of a accordingly. The modified classical inequality is $a \geq \eta$. We calibrated our triple-coincidence counting system by replacing the two-photon light source by an attenuated light bulb, and measured $\eta = 0.70 \pm 0.07$. During the data run of Fig. 3 (lower trace), we measured values of a shown at the vertical arrows. The average value of a is 0.08 ± 0.04, which violates by more than 13 standard deviations the predictions based on any classical wave theory. It is therefore incorrect to interpret these results in terms of a stochastic ensemble of classical waves, in a semiclassical theory of photoelectric detection.[21] Classical waves with conjugate, but random, frequencies could conceivably yield the observed interference pattern, but they would also yield many more triple coincidences than were observed.

We have observed Berry's phase for photons in essentially $n = 1$ Fock states, in a way which excludes with very high probability any possible classical explanation. These results can be explained in terms of the nonlocal collapse of the wave function. We conclude that this and other optical phases originate fundamentally at the quantum level, but under special circumstances, can survive the correspondence-principle limit onto the classical level.[4]

This work was supported by ONR under Grant No. N00014-90-J-1259. We thank I. H. Deutsch and A. M. Steinberg for helpful discussions, J. F. Clauser, E. D. Commins, and H. Nathel for the loan of electronics, and R. Tyroler for the loan of the Michelson interferometer.

[1]M. V. Berry, Proc. Roy. Soc. (London) A **392**, 45 (1984).

[2]B. Simon, Phys. Rev. Lett. **51**, 2167 (1983).

[3]Y. Aharonov and J. Anandan, Phys. Rev. Lett. **58**, 1593 (1987).

[4]R. Y. Chiao and Y. S. Wu, Phys. Rev. Lett. **57**, 933 (1986); A. Tomita and R. Y. Chiao, *ibid.* **57**, 937 (1986); **59**, 1789 (1987).

[5]A. Niemi, G. Semenoff, and Y. S. Wu, Nucl. Phys. **B276**, 173 (1986).

[6]R. Bhandari and J. Samuel, Phys. Rev. Lett. **60**, 1210 (1988).

[7]R. Simon, H. J. Kimble, and E. C. G. Sudarshan, Phys. Rev. Lett. **61**, 19 (1988).

[8]T. H. Chyba, L. J. Wang, L. Mandel, and R. Simon, Opt. Lett. **13**, 562 (1988).

[9]H. Jiao, S. R. Wilkinson, R. Y. Chiao, and H. Nathel, Phys. Rev. A **39**, 3475 (1989).

[10]W. R. Tompkin, M. S. Malcuit, R. W. Boyd, and R. Y. Chiao, J. Opt. Soc. Am. B **7**, 230 (1990).

[11]F. D. M. Haldane, Phys. Rev. Lett. **59**, 1788 (1987).

[12]J. Segert, Phys. Rev. A **36**, 10 (1987).

[13]M. Kugler and S. Shtrikman, Phys. Rev. D **37**, 934 (1988).

[14]Y. Q. Cai, G. Papini, W. R. Wood, and S. R. Valluri, Quantum Opt. **1**, 49 (1989).

[15]M. A. Horne, A. Shimony, and A. Zeilinger, Phys. Rev. Lett. **62**, 2209 (1989).

[16]P. G. Kwiat, W. A. Vareka, C. K. Hong, H. Nathel, and R. Y. Chiao, Phys. Rev. A **41**, 2910 (1990), and references therein.

[17]The slightly nonsinusoidal component in Fig. 3 (lower trace) can be explained by a slight wedge in $Q2$, in conjunction with the fact the signal beam was incident on $Q2$ off center.

[18]J. G. Rarity and P. R. Tapster, Phys. Rev. Lett. **64**, 2495 (1990), and references therein.

[19]C. K. Hong and L. Mandel, Phys. Rev. Lett. **56**, 58 (1986).

[20]P. Grangier, G. Roger, and A. Aspect, Europhys. Lett. **1**, 173 (1986).

[21]J. F. Clauser, Phys. Rev. D **9**, 853 (1974).